Internet of Things 25 (2024) 101060

Contents lists available at ScienceDirect

Internet of Things

journal homepage: www.elsevier.com/locate/iot

TEGBed: A thermal energy harvesting testbed for batteryless internet of things

Priyesh Pappinisseri Puluckul *, Ritesh Kumar Singh, Maarten Weyn

IDLab—Faculty of Applied Engineering, University of Antwerp—imec, Sint-Pietersvliet 7 Antwerp, 2000, Antwerp, Belgium

ARTICLE INFO

Keywords:
Energy harvesting
Internet of batteryless things (IoBT)
Internet of things (IoT)
Sustainability
Testbed
Thermal energy harvesting

ABSTRACT

This paper presents TEGBed, a testbed designed for the evaluation and testing of batteryless devices powered using thermal energy. TEGBed offers the capability to mimic real-life temperature gradients, providing researchers with a controlled environment for testing and evaluating batteryless devices. Researchers can leverage TEGBed to accelerate their investigations, gain insights into the behaviour of batteryless devices, and drive advancements in the field of sustainable and efficient IoT technologies. The TEGBed consists of a temperature emulator for emulating temperature differences, Joule Counter, a novel hardware tool for energy and power measurement, and a framework for non-supervised operation. By using the temperature emulator, TEGBed can emulate real-life energy harvesting situations in the lab. The Joule Counter allows gauging the power output from energy harvesting units for a wide range of output power. This enables researchers to gain insights into the energy harvesting capacity and efficiency of harvesting and power management units under different scenarios. With the help of different real-world use cases, we demonstrate the capabilities and effectiveness of TEGBed in assessing thermal energy harvesters and batteryless designs. In addition, we demonstrate how TEGBed can be used for the feasibility study of harvesting energy from two different underutilized heat sources; the temperature difference between soil and air and the temperature difference between the interior and exterior of a greenhouse. Emulations with the TEGBed show that, we could harvest an average of 0.89 mW power from soil-air temperature differences and 0.60 mW power from greenhouse temperature differences.

1. Introduction

The Internet of Things (IoT) has experienced tremendous growth in recent years, transforming various aspects of our daily lives through the deployment of diverse applications and devices [1]. However, a major challenge faced by IoT devices is their dependence on batteries as a power source [2]. This reliance on batteries introduces limitations such as finite battery life, the need for frequent replacements, and environmental concerns associated with battery disposal [3]. To address these challenges, energy harvesting techniques have emerged as a promising solution, enabling devices to extract and utilize energy from their surrounding environment [2].

Among the various energy harvesting approaches, Thermo Electric Generators (TEGs) have gained significant attention due to their ability to convert temperature gradients into electrical energy. TEGs offer a promising solution for powering batteryless devices, as they can leverage temperature differences in the environment to generate a continuous and sustainable power supply.

* Corresponding author.
E-mail address: priyesh.pappinisseripuluckul@uantwerpen.be (P.P. Puluckul).

https://doi.org/10.1016/j.iot.2024.101060
Received 24 July 2023; Received in revised form 6 December 2023; Accepted 3 January 2024
Available online 9 January 2024

This makes TEGs particularly suitable for applications where temperature variations are readily available, such as industrial settings, transportation systems, and even human body heat [4].

In this paper, we introduce TEGBed, a testbed specifically designed for the evaluation and testing of batteryless devices within the context of the Internet of Batteryless Things (IoBT). TEGBed stands as an innovative emulation tool that allows researchers to assess the performance and viability of batteryless devices under realistic conditions, without the need for actual field deployments. By accurately replicating temperature gradients that mimic real-life situations, TEGBed enables comprehensive evaluation of batteryless devices' behaviour and functionality. Moreover, by simulating real-life conditions, researchers can gain valuable insights into the energy harvesting efficiency, power consumption, and overall performance of batteryless devices. This allows for in-depth analysis, optimization, and validation of different batteryless device architectures, algorithms, and energy management strategies, paving the way for sustainable and autonomous IoT deployments.

In summary, the growth of IoT has necessitated energy harvesting techniques to overcome battery constraints. Testbeds can provide a controlled environment for evaluating and testing batteryless devices. Furthermore, advancements in TEG characterization and temperature control have enhanced the accuracy and dependability of energy harvesting systems, facilitating progress in sustainable and efficient IoT technologies. The subsequent sections of this paper present TEGBed as a means to acquire valuable insights into the behaviour of batteryless devices and validate the practicality of thermal energy harvesting through real-world data. TEGBed, unlike many other testbeds presented so far [5–8], is not intended for evaluating and analysing TEG modules alone. Instead, it targets the whole batteryless and energy-harvesting system architectures. Evaluating a power management unit requires driving it to its maximum efficient load and gauging sub-milliwatt power from the energy harvesting unit. This often demands sensing of ultra-low harvester currents in the sub-microampere range. Sensing such ultra-low current levels is a challenging process and requires complex and careful hardware design. TEGBed, with the help of Joule Counter, a capacitor-based energy gauging tool, enables the measurement of extremely low energy and power output without compromising accuracy. In addition, by integrating a software framework, TEGBed has been moulded as an automated and non-supervised testbed.

In this paper, we present the following contributions:

- Design and Development of TEGBed: We discuss the design and development of TEGBed, an emulator specifically designed for evaluating batteryless IoT devices powered by thermal energy harvesting. TEGBed offers the capability to accurately emulate a wide range of temperature gradients, allowing researchers to assess the performance of batteryless devices under various energy harvesting conditions.
- Joule Counter: We introduce a hardware tool called Joule Counter, which enables the realtime recording of energy and power output from the device under test. This tool provides valuable insights into the energy harvesting efficiency of the tested devices, allowing for comprehensive analysis and optimization.
- Emulation Controller: We develop an Emulation Controller, a framework that facilitates the non-supervised operation of TEGBed. The Emulation Controller streamlines the testing process by automating various tasks and enabling long-term evaluation of energy harvesting and batteryless devices without any manual intervention.
- Case Study of Thermal Energy Harvesting: We present four detailed case studies that showcase the effectiveness of thermal energy harvesting using real-world data. Through this case study, we explore the possibilities of powering different LPWAN standards using thermal energy harvesting techniques, demonstrating the potential practical applications of this technology.

The rest of the paper is organized as follows. Section 2 explains the motivation and necessity for this work in contrast to state-of-the-art. Section 3 includes a detailed discussion of the architecture of the testbed. Section 4 analyses and explains some potential use cases of TEGBed. It thoroughly discusses the characteristics of applications and validates using two real-time studies. Section 5 adds the in-line discussion outlines the future work and Section 6 summarizes our contribution.

2. Related work

The increasing demand for low-power wireless sensors in the rapidly growing IoT has brought a heightened focus on the need for energy harvesting. Traditional battery-powered devices pose lifespan and network performance challenges, making energy-harvesting technology a promising solution. In [9], recent advances in energy harvesting techniques for IoT have been reviewed, highlighting the practical advantages and case studies of energy harvesting. Despite being a promising solution, there are still many research challenges to address for the large-scale deployment of energy-harvesting solutions in IoT environments. The continuous operation of battery-powered devices is a challenge, especially in remote locations where battery replacement is difficult. Paper [10] focuses on surveying energy harvesting techniques that aim to enhance the lifetime of IoT devices by harnessing environmental energy as a sustainable power source. In addition, the survey [11] provides insights into the advancements, challenges, and case studies related to energy harvesting techniques for IoT devices, laying the foundation for future research and development in this field.

Batteryless IoT has gained significant attention due to the growing need for sustainable and maintenance-free IoT deployments. The paper [12] focuses on the design and development of a novel energy harvesting and power management system for battery-less IoT devices. The study proposes a hybrid energy harvesting approach that combines solar and RF energy sources, along with an efficient power management scheme to maximize the harvested energy utilization. In another paper [13], the authors investigate the use of ambient RF energy harvesting for powering IoT devices. They propose an RF energy harvesting system that utilizes an adaptive power control mechanism to optimize energy extraction from the RF environment. The study presents simulation results showing the feasibility of RF energy harvesting as a viable power source for battery-less IoT devices. Furthermore, the paper [14] explores the

application of energy harvesting techniques for ultra-low power IoT devices. The authors present a comprehensive review of energy harvesting technologies, including solar, RF, and thermal energy, and discuss their suitability for powering battery-less IoT devices. The study highlights the importance of efficient power management techniques and provides insights into the challenges and future directions in the field of energy harvesting for emerging battery-less IoT. These advancements pave the way for sustainable and self-powered IoT devices, eliminating the need for traditional batteries and enabling long-term operation in various applications.

The recent focus on energy management and efficiency has sparked interest in thermoelectric generators, enabling the recovery of lost thermal energy and power generation in extreme environments. The review paper [15] focuses on vibrational and thermal energy harvesters, explaining their working principles and configurations. It highlights the progress, advantages, and potential applications of hybrid energy harvesting systems in infrastructure monitoring, industry conditions, transportation, healthcare, marine systems, and aerospace engineering. Another review paper [4], explores the principles of thermoelectricity along with the discussion on existing and future materials and addresses thermoelectric generator design and optimization. The paper underscores the importance of considering thermoelectric generators whenever heat transfers from a hot to a cold source, showcasing their wide-ranging applications in industry and domestic settings.

One of the use cases discussed in [16] addresses the feasibility of using TEGs to harvest energy from heat loads within satellites by developing an assistance system for satellites to enable communication and data transmission for deorbiting maneuvers. These types of applications need a testbed to do analysis before real deployment to investigate material, harvested energy, and other factors. Another paper [17], highlights the wide range of materials, including organic, hybrid organic–inorganic, and presents design considerations and real-world applications. This comprehensive overview highlights the potential of thermoelectric materials in powering future ubiquitous devices. Wearable devices can also leverage body heat for thermoelectric energy harvesting. The paper [18] explores thermoelectric energy harvesting on individuals, finding that power generation is independent of metabolic rate. An integrated energy-harvesting system in an office-style shirt produces substantial power, outperforming alkaline batteries of similar size and weight over an extended period. Current research focuses on improving material properties and Thermoelectric Module (TEM) design. However, integrating the TEM with a DC–DC converter is essential for optimal performance [8]. The interaction between the TEM and converter affects power generation efficiency, requiring accurate simulation models for system design. The paper [19], highlights the need for a testbed to demonstrate the practical feasibility of the simulation model for real-world experimentation. By utilizing the testbed, the researchers validate the accuracy and effectiveness of the proposed model, showcasing its practical applicability.

The performance of energy harvesting systems relies heavily on the unpredictable nature of the environment. Paper [20] introduced a testbed for evaluating energy harvesting systems in a controlled environment. The testbed enables precise and repeated testing of the system using thermal and radiative sources while accommodating arbitrary current profiles. By coordinating boundary conditions, it allows detailed exploration and evaluation of energy management and harvesting systems. With accelerated reproduction of environmental traces, the testbed significantly reduces evaluation time, ensuring fast and consistent assessment across diverse operating conditions. Further, [5] is focused on an experimental investigation of a TEG to harness electric energy from temperature gradients in CubeSat solar panels. The study analyzes the TEG's generation capacity based on different positioning configurations and evaluates its performance using two distinct energy harvesting circuits. Another paper [21] presents the design and instrumentation of a 3:5-scale physical testbed of an intelligent building for evaluating temperature control algorithms. It features controlled mass flow, a sensor-rich environment, adjustable ambient temperature, and a modular structure. The testbed's unique placement within a larger temperature-controlled enclosure enables the simulation of time-varying ambient weather conditions. In addition to the necessity of a testbed, there is significant scope for discussing the characterization of TEGs and electronic circuits. The work in paper [6] demonstrates the system with high precision and accuracy, enabling the acquisition of various TEG characteristics such as internal resistance, open circuit voltage, power output, and temperature gradient. Another work [7], employs a measurement setup using thermistors instead of thermocouples and a simplified component configuration, where temperature measurement uncertainty is significantly reduced. This advancement enables millidegree-precision temperature control and enhances the accuracy of temperature-derived measurements by two orders of magnitude.

TEGBed, a testbed for batteryless devices powered by thermal energy harvesters, presented in this paper contributes to the advancement of batteryless IoT devices powered by thermal energy harvesting, providing researchers and system designers with valuable tools, frameworks, and insights for enhancing device performance and energy efficiency. By enabling accurate measurement of sub-milliwatt level energy output using Joule Counter, TEGBed provides a near real-world situation for analysing energy harvesting designs. In addition, its ability to replay and mimic data from real-world deployments makes it a suitable solution for testing and evaluating batteryless designs. In the following sections, we delve into the details of TEGBed architecture and its capabilities.

3. TEGBed architecture

The TEGBed is intended for re-creating real-life situations in the lab to evaluate the performance of thermal energy harvesting devices. A diagrammatic representation of the TEGBed architecture is presented in Fig. 1. A photo of the TEGBed is shown in Fig. 2. In the following sections, we provide an in-depth discussion of the individual components of the TEGBed.

As shown in Fig. 1, an Emulation Controller (EC) is the control unit of the testbed which controls and manages the entire testbed. Further, the architecture contains two temperature controllers and two heaters/coolers for creating the thermal energy harvesting conditions. The device under test (DUT) or TEG is sandwiched between these two heaters/coolers. Finally, a Joule Counter or Joulescope can be used to evaluate the system under different test conditions. A solid line in Fig. 1 indicates a default connection while a dashed line indicates an alternate connection. The control lines are represented using blue lines whereas the voltage (current) paths are indicated with red lines.

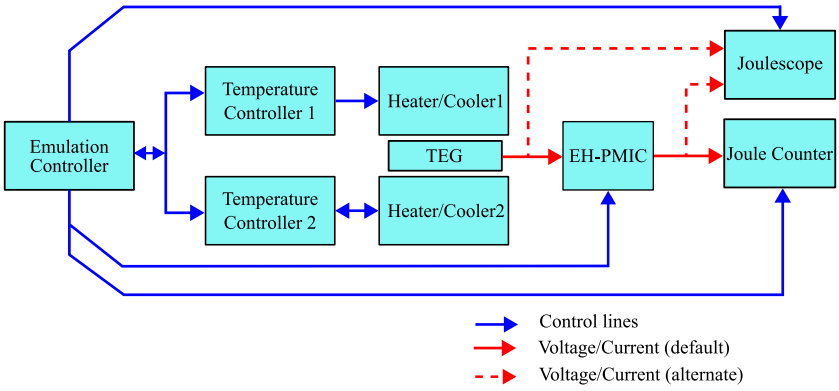

Fig. 1. A block diagram representation of the TEBed architecture.

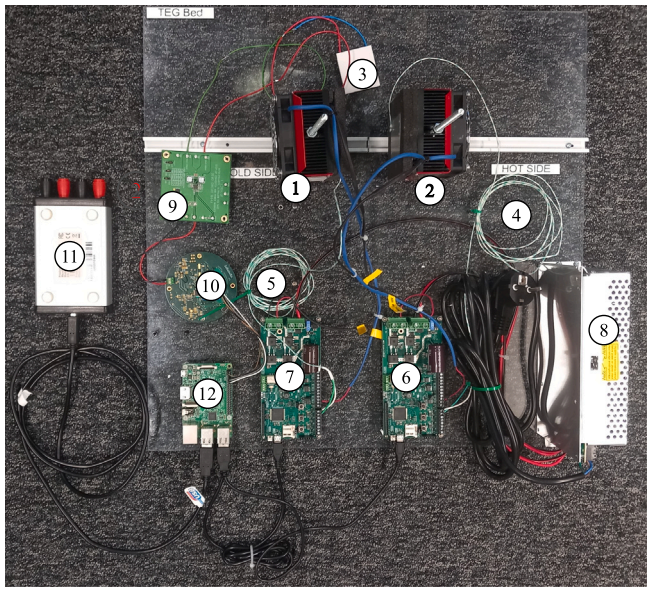

Fig. 2. A photo of the TEGBed. ①, ② Heater/Cooler ③ TEG to be tested ④, ⑤ K-type thermocouples for temperature sensing ⑥, ⑦ PID controllers ⑧ Power supply for heaters/coolers, ⑨ LTC3109 PMIC ⑩ Joule Counter ⑪ Joulescope ⑫ Single Board Computer.

3.1. Temperature emulation

The core of the TEGBed architecture is the temperature emulator, which can produce the desired temperature difference across the TEG under test. The temperature emulator consists of two Peltier elements which can either cool down or heat up the point of contact. We use Direct-to-Air type thermoelectric heating/cooling device DT-AR-034-12 from European Thermodynamics to generate temperature differences [22]. In addition to this, two temperature controllers, one for each temperature generator, are used to control and maintain the temperature at desired set points. PID temperature controllers from Adaptive Thermal Management are employed for this purpose [23]. The controllers use K-Type thermocouples to read the temperature of the generator and maintain the set point using the PID feedback algorithm. The PID controller has an accuracy of ±0.5 °C. By using the USB interface provided, the temperature controllers can be remotely configured and managed.

3.2. Joule counter

A crucial requirement in assessing the efficiency of energy harvesting systems is the accurate measurement of energy and power outputs under different conditions. Often, resistor-based power measurement tools are used for this. This involves introducing a shunt resistor between the harvester and the load and measuring the current through the load. However, this method requires a matching load to be connected to ensure maximum power transfer. Moreover, often complex and accurate circuits are required to

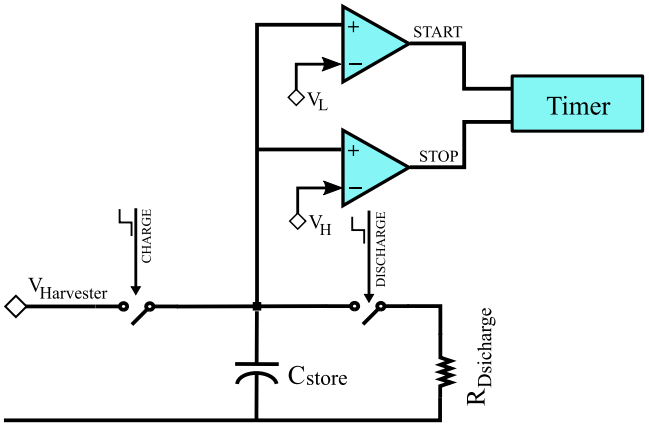

Fig. 3. A schematic diagram of the Joule Counter circuit used to measure the energy output from the energy harvesting unit.

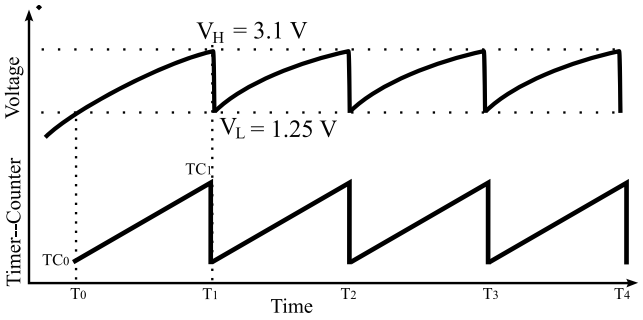

Fig. 4. Charge discharge cycle of the capacitor C_{store}.

measure load currents in a wide range. Otherwise, the circuit should be able to adjust the load until the maximum power point is achieved. This paper introduces Joule Counter, an energy measurement tool that can operate over a wide range of load currents. The Joule Counter is a calibrated energy measurement tool that can be used to accurately assess the amount of energy produced by the TEG under test. Joule Counter measures energy by charging and discharging a capacitor between two pre-set voltage levels. For any capacitor charged to a voltage V, the energy can be calculated as $E = \frac{1}{2}CV^2$. Therefore, if we know the capacitance and voltage level, we can calculate the energy stored in the capacitor. In addition, if we know the charging time, then the average power can be estimated. The Joule Counter uses this principle to gauge the energy and power produced by the energy harvesting system. However, the chosen capacitor must be able to withstand the peak power output from the charging source. We define two voltage thresholds for charging and discharging the capacitor, a lower threshold V_L and a higher threshold V_H. Two comparators as shown in Fig. 3 are employed to monitor the voltage levels of the capacitor, one with reference voltage V_H and the other with reference voltage V_L. In Fig. 4, when the capacitor voltage crosses V_L at time T_0, the first comparator fires a timer. The timer keeps track of the charging time of the capacitor until the capacitor voltage reaches the threshold V_H at time T_1. On hitting V_H, the second comparator turns the timer off. Reading the timer value, $TC1$ at this time gives the time taken by the energy harvester to charge the capacitor from V_L to V_H. The capacitor is then discharged via a resistor $R_{Discharge}$ to prepare for the next measurement cycle. By using the capacitor energy equation, the energy transferred to the capacitor for the time $T_1 - T_0$ can be written as,

$$E_{store} = \frac{1}{2}C_{store}(V_H^2 - V_L^2) \tag{1}$$

The average power output from the energy harvester can be calculated as,

$$P_{harvester} = \frac{E_{store}}{T_1 - T_0} \tag{2}$$

The Joule Counter uses an STM32L072 ARM processor from STMicroelectronics [24] to implement its state machine. The low power timer of STM32L072 which is configured with a time base of 50 µs measures the charging time. Two internal comparators *COMP1* and *COMP2* are used for threshold detection. *COMP1* is configured with a reference voltage of 1.25 V and *COMP2* with 3.1 V. Low-power switches SiP32432 [25] controlled via the *IO* lines are used to manage the charging and discharging of the capacitor. Two 220 µF ceramic capacitors connected in parallel are used as C_{store} [26], giving a total capacitance of 440 µF. A 10 kΩ resistor is used in the discharge path to limit the current while discharging C_{store}. The timer is turned on and off based on the signals from the

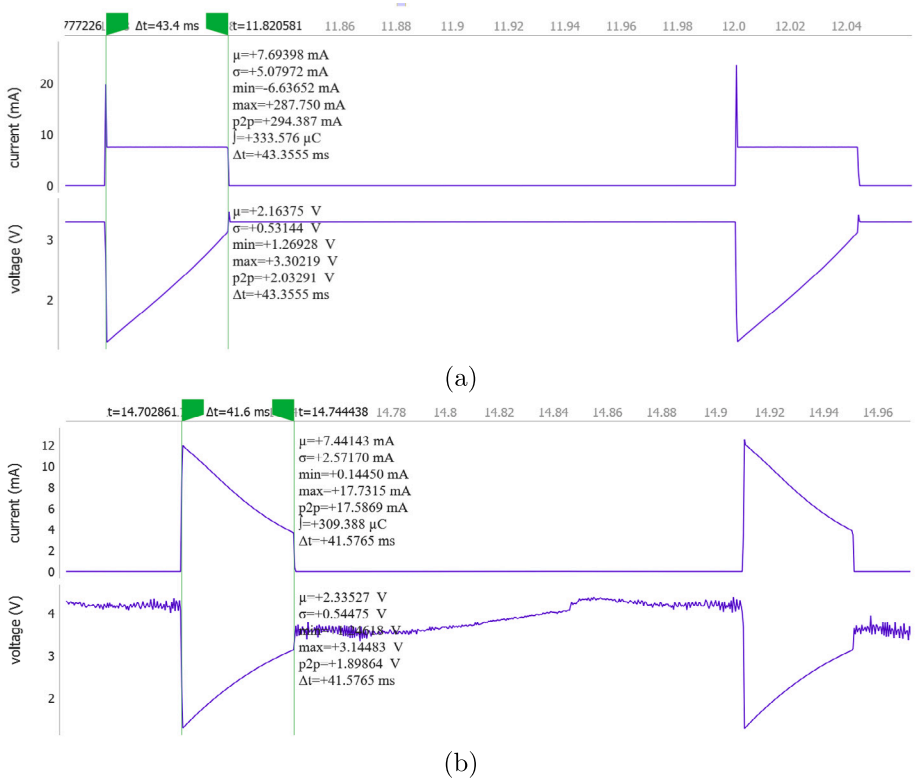

Fig. 5. Current and voltage curves of the Joule Counter captured using Joulescope for (a) constant current charging and (b) constant voltage charging. Constant current charging measures an average voltage of 2.16 V and an average current of 7.69 mA for a charging time of 43.35 ms giving a total stored energy of 720.51 μJ. The constant voltage charging measures an average voltage of 2.33 V and an average current of 7.44 mA for a charging time of 41.57 ms giving a total stored energy of 720.28 μJ.

comparators. Once the timer is stopped, the ARM processor reads the charging time and sends it out via a *UART* interface. Since we already know the energy transferred to C_{store}, average power can be calculated using the charging time and energy value.

The Joule Counter provides an easy way to estimate energy output from the emulator. However, power calculated using Eq. (2) could be impacted by noise. This mainly involves drift in the timer's clock and variations in the value of C_{store} with temperature and bias voltage. Variations in C_{store} with temperature may be ignored since the emulator works at room temperature. However, the dependency of capacitance on bias voltage and clock drifts must be considered. Consequently, calibration is required to ensure accurate readings from the Joule Counter.

Calibrating the Joule Counter involves two steps, correcting the capacitance C_{store} and then correcting for the time and energy drift. A correction for the capacitance is required since we use a ceramic capacitor. A ceramic capacitor's capacity varies with bias voltage. Thus, we first establish an accurate value of the capacitance for the working voltage range of C_{store}. To accomplish this, pre-defined charging current and voltage are fed to the Joule Counter, and the energy flow is measured using a Joulescope [27]. V_H and V_L are set to be 3.1 V and 1.25 V respectively. We measure the energy transfer to the capacitor for both constant current and constant voltage modes. Screenshots of the Joulescope measurements for both modes are shown in Fig. 5. The Joulescope measurements show that C_{store} was charged to 309.38 μC with an average voltage of 2.33 V in constant voltage mode and 333.57 μC with an average voltage of 2.16 V in constant current mode. Or, the capacitor stored $E_{store} = 720.51$ μJ of energy. By using the values of E_{store}, V_H and V_L we recalculate the value of C_{store} as 178.86 μF.

Once the actual value of C_{store} is derived, the accuracy of the Joule Counter measurements needs to be evaluated. For this, the Joule Counter was subjected to charging currents starting from 150 μA to 10 mA using Keysight's N6705B power analyser [28]. The power analyser was configured in constant current mode, and 100 readings (charging time) were recorded for each charging current and, the average value was calculated. A plot of actual charging time against measured charging time is shown in Fig. 6(b). Actual charging time is calculated using the equation $I = C\frac{dv}{dt}$. Since C, dv and I are fixed, dt can be calculated. As given in Eq. (2), the average power measured by the Joule Counter is inversely proportional to the charging time. Since the value of E_{store} is a constant, the error in average power is determined by the accuracy of the measured charging time. For instance, an error of 1 ms, when the input power is 25 mW can introduce an error of around 800 μW in the estimated power. From Fig. 6(a), we can conclude that the time measured by the Joule Counter deviates from the actual value by around 17 ms at 0.15 mA and around 0.5 ms at 10 mA. This translates to an error of 2.9 μW and 320 μW respectively. Therefore, the error needs to be corrected to ensure trustful readings from

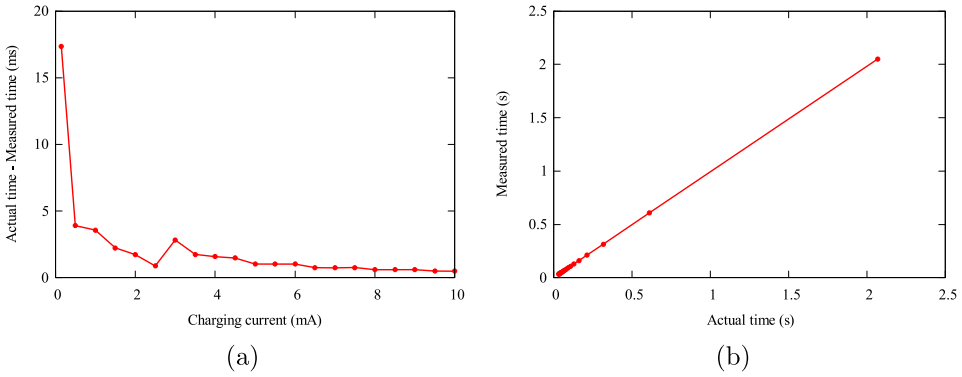

Fig. 6. Calibration of the time base of the Joule Counter. (a) Difference between the time measured by the Joule Counter and actual time at different charging currents. The error in Joule Counter measurements is directly proportional to the error in time measurements. (b) measured time plotted against actual time at different charging currents.

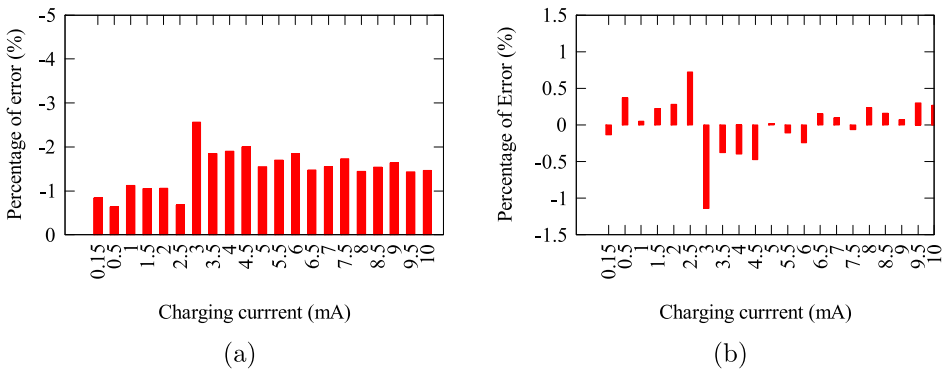

Fig. 7. Percentage of error in charging time measured by Joule Counter compared to actual values. (a) without regression (b) after regression.

the Joule Counter. We use the regression method to reduce the error in the measurements. Though the linear regression method looks apt to this solution based on the relation depicted in Fig. 6(b), we found power regression to perform better than linear regression. Power regression can be written as,

$$y = A.B^{x} \tag{3}$$

where A and B are regression coefficients. y is the dependant variable and x is the independent variable. The measurement from the Joule Counter is used as the dependent variable, and the actual discharge time calculated is used as the independent variable. On solving for the values of A and B, we derive A = 1.0089 and B = 0.997 respectively. The percentage of error in the measurements after and before linear regression is shown in Fig. 7.

3.3. Energy harvester power management unit

The output from the TEG is usually in millivolts, which is insufficient to power an electronic circuit directly. To boost the voltage output from the TEG to a usable range, a Power Management Integrated Circuit (PMIC) is required. TEGBed uses LTC3109 from Analog Devices for this purpose [29]. LTC3109 can work with an input voltage as low as 30 mV. It has multiple output voltage levels which the designer can choose, and it can tickle charge a supercapacitor. Beyond these features, LTC3109 is equipped with an auto-polarity detector, which makes the functioning of the PMIC independent of the polarity of the TEG voltage. This is an incredibly useful feature since the output of the TEG can change its polarity depending on the temperature gradient. The TEG modules usually have two sides, designated as cold and hot. The polarity of the output voltage depends on which side of the TEG is at a higher temperature.

The boosted voltage from the TEG is connected to the Joule Counter, which can then estimate the energy production capability of the TEG. In addition to this, a Joulescope may be connected between the PMIC and TEG or between the PMIC and Joule Counter to measure the current and input voltage into the PMIC or the Joule Counter. The Joulescope is a precision DC energy analyser that can accurately measure current and voltage in a wide range and estimate the power and energy of extremely low-power devices [27]. Joulescope is useful in situations where the energy flow into a load needs to be measured, for instance when testing a batteryless design. On the other hand, the Joule Counter terminates the circuit and can only be used to measure the energy production capacities of an energy harvesting unit.

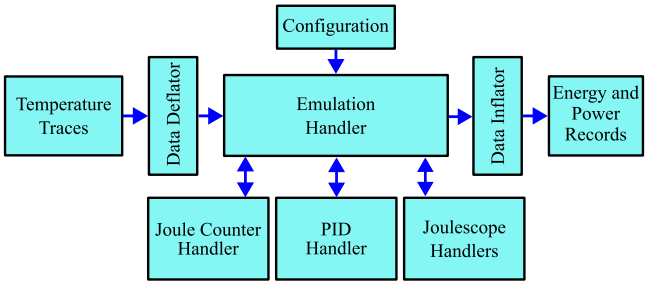

Fig. 8. A block diagram of the Emulation Controller software.

3.4. Automated emulation and testing

The TEGBed is steered by an Emulation Controller (EC) running on a Raspberry Pi Single Board Computer (SBC). The EC includes a set of Python scripts that interacts with the hardware components of the TEGBed including Joule Counter, Joulescope and the temperature emulators and controls them to ensure an automated simulation process. A simplified block diagram of the EC software architecture is shown in Fig. 8. The emulation process involves controlling the cold and hot side temperatures of the TEG using temperature generators. Once the temperatures at the hot and cold sides of the TEG stabilize at the required set points, the Joule Counter or the Joulescope has to be activated to gauge the energy output. This whole process is automated with the Emulation Controller.

To conduct an emulation, the EC requires details of the temperature differences to be generated. This should be provided as a CSV file with timestamps, hot side temperatures and cold side temperatures specified. The CSV file can have either mock data or data collected from real-life deployments. The mock data set is useful when the user wants to put the device under a wide range of test conditions and assess its performance. Whereas a real-life data set is useful for reproducing the real-life conditions in the lab and then monitoring the performance of the device. For instance, this could be used to reproduce a device failure that happened with the deployed device. Then with the help of TEGBed, the same condition as well as failure can be reproduced in the lab. In addition to the data set, a configuration file for the emulation experiment needs to be supplied. The configuration file specifies the type of emulation, sequence number of the emulation and the destination and source directory for the input data and results. As stated earlier, the TEGBed can be used for either evaluating the power generation capability of a specific energy management unit under different conditions or to evaluate an overall batteryless design. The type of experiment in the configuration file provides this detail to the EC so that it can choose either the Joule Counter or the Joulescope for recording the results. The entire emulation is supervised by an Emulation Handler. The Emulation Handler interacts with each hardware tool using their respective handlers. Once the CSV file is loaded, the Emulation Handler parses the file and launches an Emulation. The experiment runs until all the temperature gradients specified in the CSV files are applied sequentially, and the Joule Counter or the Joulescope values are recorded.

The total emulation time is mostly dependent on the number of temperature samples to be played by the TEGBed. In many situations, the size of the sample file may be significantly large. For instance, the temperature traces collected from environments can be many days long. Consequently, the time taken by the TEGBed will increase. To mitigate this issue, a data deflator is used. The data deflator reduces the number of samples by removing repeating data points in the data set. So, instead of the whole data set, the emulation can be conducted for a significantly smaller set. Once the emulation for the deflated data set is finished, a data inflator is used to recreate the original data and results. However, it must be noted that the deflator–inflator is useful only in emulations intended for estimating the generated power from an energy harvester unit and not in analysing batteryless designs. We discuss the data inflator and deflator in detail in Secton 4.

4. Applications and use cases

TEGBed offers a straightforward architecture that can enable the evaluation of a wide range of batteryless designs powered by thermal energy. In this section, we focus on four distinct use cases and elaborate on how TEGBed can help to asses these specific applications. Through extensive emulations and analysis with TEGBed, we examine the feasibility and efficiency of each use case. We expect these case studies to provide the research community with valuable insights and practical know-how on the application of TEGBed to evaluate divergent thermal energy harvesting applications.

4.1. Power output evaluation of thermal energy harvesting system at low-temperature gradients

TEG modules are efficient in generating energy only if there is a significant temperature difference across them. They are notoriously inefficient at low-temperature differences. Despite the inefficiency, TEGs are innovatively used in many use cases where extremely low-temperature differences are available [30,31]. Details on the performance and characteristics of TEG modules are crucial in selecting the right module for an application. However, for these low-power applications, data sheets from the

Table 1
TEG modules used for evaluating energy production capacity at low-temperature differences.

Manufacturer	Part no.	Width (mm)	Length (mm)	Height (mm)
ETDYN	GM200-127-14-16	40.0	40.0	3.40
Marlow	TG12-6-01L	40.13	40.13	3.91
Marlow	TG12-4-01LS	30.00	30.00	3.33

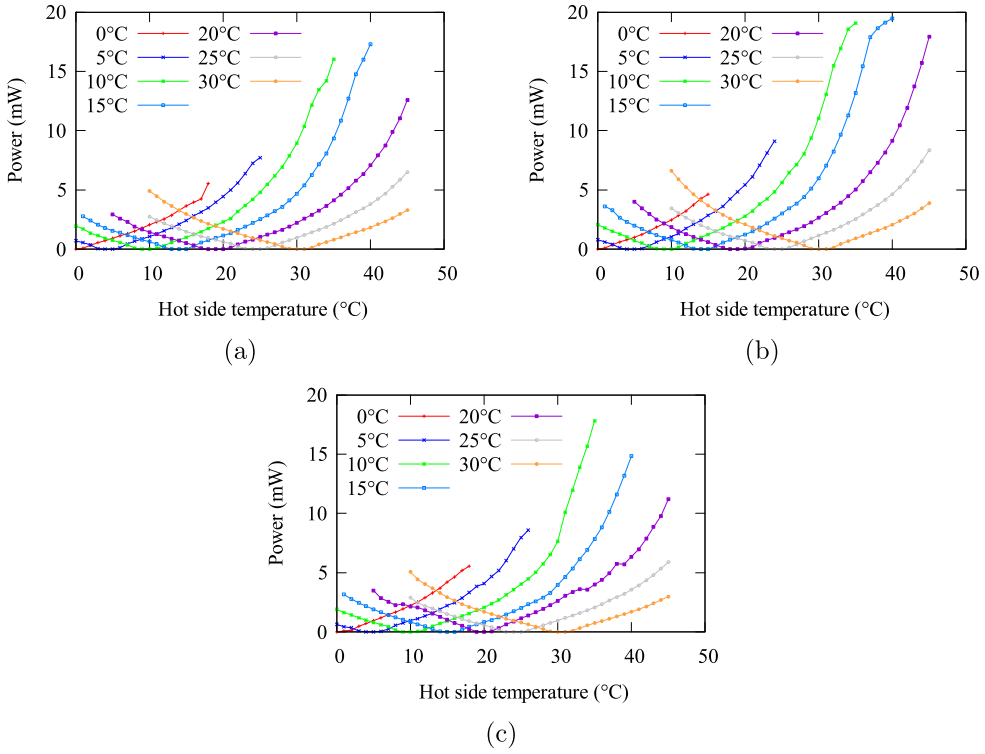

Fig. 9. Comparison of power output for the three modules. The hot and cold sides of the modules were subjected to different temperatures using TEGBed, producing a temperature difference from 1 °C to 25 °C across the TEG. The TEGBed then recorded the power output for every temperature for each module. (a) GM200-127-14-16 (b) TG12-6-01L and (c) TG12-4-01LS.

manufacturers have limited details. We show, how TEGBed with its ability to generate extremely low-temperature gradients can be used to evaluate the performance of thermal energy harvesting systems at low-temperature gradients. We chose three commercially available TEG modules and assessed their performance at different temperature gradients. For each module, seven sets of experiments were conducted. The hot side temperature (T_{hot}) was incremented by 5 °C in each set, starting from 0 °C. The cold side temperature (T_{cold}) was adjusted from 0 °C to, 45 °C depending on the hot side temperature. The maximum and minimum differences applied across the modules were 0 °C and 25 °C. For every temperature difference, the TEGBed measured the energy and power outputs. The details of the modules used for the study are listed in Table 1.

The characteristics of all three modules as recorded by the TEGBed for different temperature differences are shown in Fig. 9. The curves show a bell shape since we applied both negative and positive temperature differences to the modules. A negative temperature means that the cold side of the TEG is at a higher temperature than the hot side. Ideally, a change in temperature polarity should not impact the output of the module. For instance, the module GM200-127-14-16 from European Thermodynamics does not designate any side as hot or cold. Whereas the modules from Marlow Industries have the sides specifically labelled as hot and cold. Therefore, we expected a symmetrical power curve against temperature differences. However, we observe that there is some difference between the power outputs at a temperature difference and its negative. We noted the same behaviour in the results produced by all three modules. Thus, we attribute it to the power management circuit. Since the PMIC uses a polarity detector circuit to deal with temperature reversals, we expect this to affect the power generated when the temperature difference changes its polarity.

In Fig. 10, the modules are compared for power generation capabilities at different temperature differences. A negative temperature on x-axes indicates that the cold side was at a higher temperature than the hot side. In our experiments, we observed that the power produced is higher when $T_{hot} > T_{hcold}$ compared to $T_{hot} < T_{cold}$. From the comparison in Fig. 10, it is clear that module TG12-6-01L has a higher energy conversion capability compared to modules TG12-6-01L and TG12-4-01LS. However, it

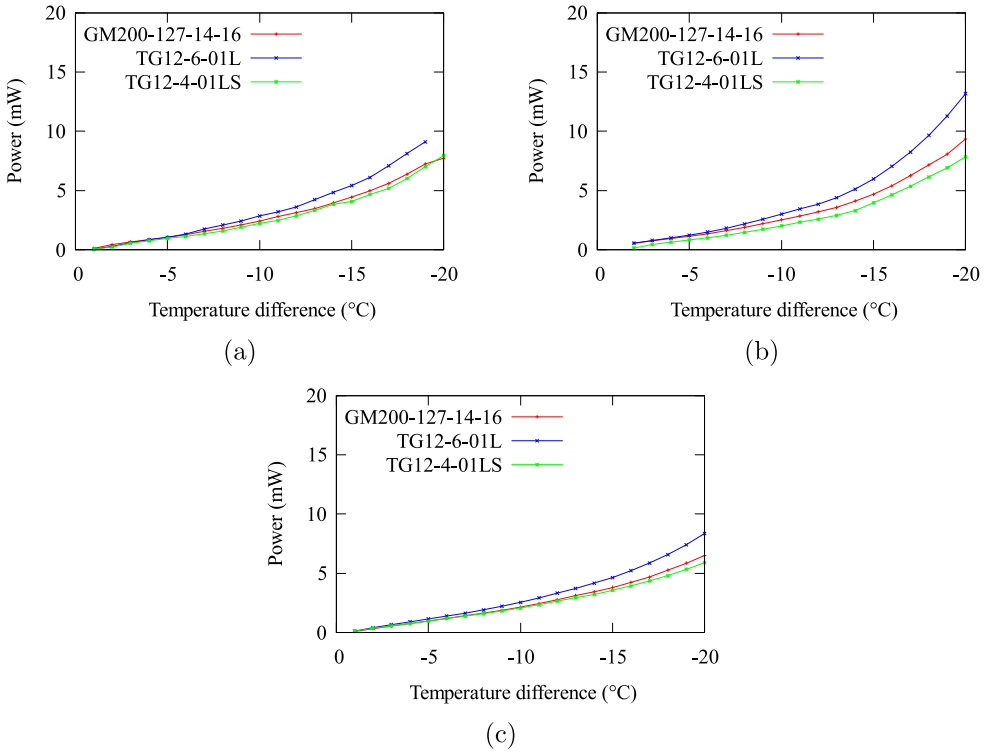

Fig. 10. Comparison of power generated by TEG modules GM200-127-14-16, TG12-6-01L and TG12-4-01LS for temperature gradients from 1 °C to 20 °C at different hot side temperatures. (a) T_{Hot} = 5 °C (b) T_{Hot} = 15 °C (c) T_{Hot} = 25 °C. The negative sign indicates that the hot side temperature is lower than the cold side temperature.

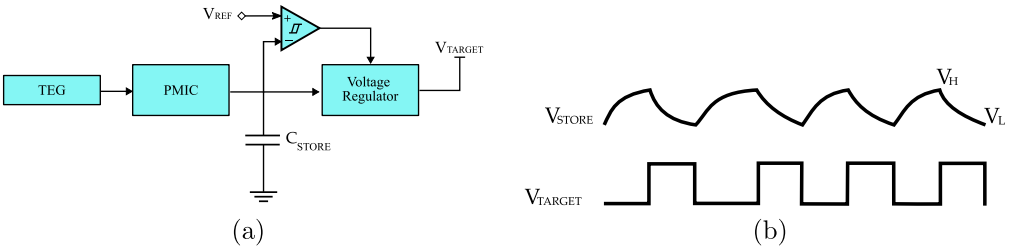

Fig. 11. A batteryless IoT device. (a) basic architecture (b) supercapacitor charging and discharging and target voltage levels.

is worth noting that the TEGBed does not directly measure the power produced by the TEG, but after converting it into a usable voltage range by the PMIC. Thus, the results show the overall performance of the TEG and the PMIC. Usually, the details on the efficiency of the PMIC are available from respective datasheets. So, it is possible to extract the power output of the TEG module alone by compensating for the losses introduced by the PMIC. Nonetheless, since an energy harvesting unit combines a TEG and PMIC, we consider the overall efficiency as the major deciding factor. As stated earlier, currently we use LTC3109 PMIC for power management. However, the users can replace it with their own PMIC or a custom power management unit.

4.2. Evaluating batteryless IoT design with TEGBed

In this section, we discuss how TEGBed can be used to evaluate batteryless IoT designs. Batteryless devices often use the architecture as shown in Fig. 11(a). The device uses a PMIC for power management and stores the generated energy in a supercapacitor. The voltage of the supercapacitor is regulated using a voltage regulator before powering the target. The target device would involve many components such as sensors, a real-time clock, a microcontroller, a communication module, etc. The voltage regulator is required since the supercapacitor's voltage varies with the charge–discharge process. Usually, a switching regulator serves as the voltage regulator capable of maintaining stable output within a range of input voltages. Additionally, a comparator

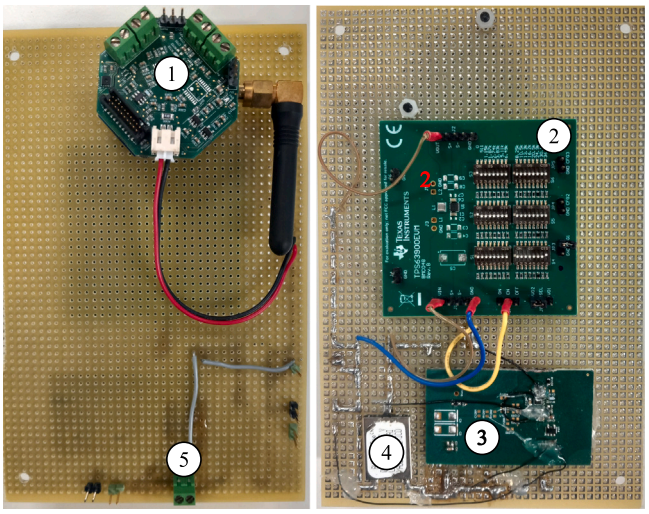

Fig. 12. Pictures of the batteryless DASH7 node used ① DASH7 node ② TPS63900 buck-boost converter ③ supercapacitor voltage monitoring circuit ④ 33 mF supercapacitor, ⑤ connector for the output from energy harvesting PMIC.

with hysteresis is used to enable and disable the voltage regulator based on the voltage levels of the supercapacitor. The comparator has two thresholds, a low threshold V_L, and a high threshold V_H. As, long as the supercapacitor voltage is within these levels, the voltage regulator is active as shown in Fig. 11(b). Due to the inherent losses in the voltage regulator, only a portion of the energy stored in the capacitor gets transferred to the load.

The selection of the right value of energy buffer plays an important role in the design of any batteryless design. The crucial point to remember while choosing an energy buffer is that it should be able to serve the target during the execution of its peak energy-consuming state. Thus, it can be written that,

$$\eta.E_{STORE} \geq E_{Peak} + E_{leakage} \tag{4}$$

where $E_{STORE} = \frac{1}{2}C_{STORE}(V_H^2 - V_L^2)$ is the energy stored in the capacitor, η is the efficiency of the voltage regulator and E_{Peak} is the peak energy consumption of the target. The regulator efficiency accounts for the energy lost during the voltage conversion process. Hence, the minimum value of the buffer is decided by the highest energy-consuming activity of the target and can be written as,

$$C_{min} = 2.\frac{E_{Peak} + E_{leakage}}{\eta(V_H^2 - V_L^2)} \tag{5}$$

In a batteryless design where the target executes its tasks sequentially after waking up, selecting $C_{STORE} = C_{min}$ guarantees a successful execution of the target for every charging of capacitor to V_H. For instance, a wireless temperature sensor would sense the temperature and transmit the data every time it wakes up. However, when $C_{STORE} = C_{min}$, the frequency of execution of the tasks is solely determined by the energy harvesting rate. It is worth noting that, if the system executes its tasks in a non-sequential manner, the capacity of the storage buffer is decided by many other factors such as the priority of the task, energy consumption of the task, etc. [32,33].

To evaluate the effectiveness of TEGBed in emulating energy harvesting situations for testing batteryless devices, we built a batteryless device, which is shown in Fig. 12. The device uses a DASH7 [34] communication module to transmit data from a temperature and humidity sensor. In addition, a nano-watt buck-boost regulator TPS63900 is used to regulate the voltage to the target. A comparator circuit with $V_H = 3.3$ V $V_L = 2.5$ V and designed using TLV3691 [35] is used to monitor the voltage levels of the energy buffer. The output from the TEGBed is fed to the device via the input connectors.

The minimum capacitance, C_{min} required for the batteryless DASH7 design, can be calculated using equation Eq. (5). For this purpose, the energy profile of the target was acquired using the Joulescope and is depicted in Fig. 13. The energy consumption for the target execution was measured to be 47.6 mJ. Further, we chose $V_H = 3.3$ V and $V_L = 2.5$ V and $\eta = 90\%$. We assumed energy loss due to leakage $E_{leakage}$ negligible and hence not included in the calculation. Substituting these values in Eq. (5) yields, $C_{min} = 22.51$ mF. However, since we did not have the exact value of the supercapacitor available in our inventory, we selected the nearest value available. Thus, a 33 mF capacitor from Kyocera was used as C_{STORE} [36]. A 33 mF has room for more than the required amount of energy to perform one sensing and transmission.

To examine and assess the batteryless DASH7 design, temperature differences starting from 1 °C to 10 °C were generated using TEBed. The TEG module TG12-6-01L from Marlow Industries was used as the energy generator. The Joule Counter was disconnected and replaced with the Joulescope to monitor the energy flow to the target device. For each temperature difference, we ran the experiment for 1 h. The voltage of the supercapacitor and the task execution of the target were continuously monitored. The target, once powered on, performs a sensor measurement and immediately transmits the acquired data. If there is enough power available,

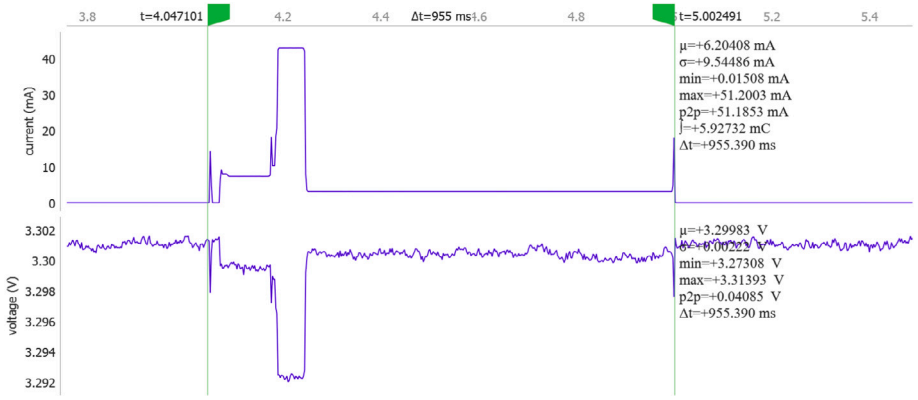

Fig. 13. Energy profile of the DASH7 target node captures using Joulescope. The profile shows startup, sensing, transmission, and data processing activities.

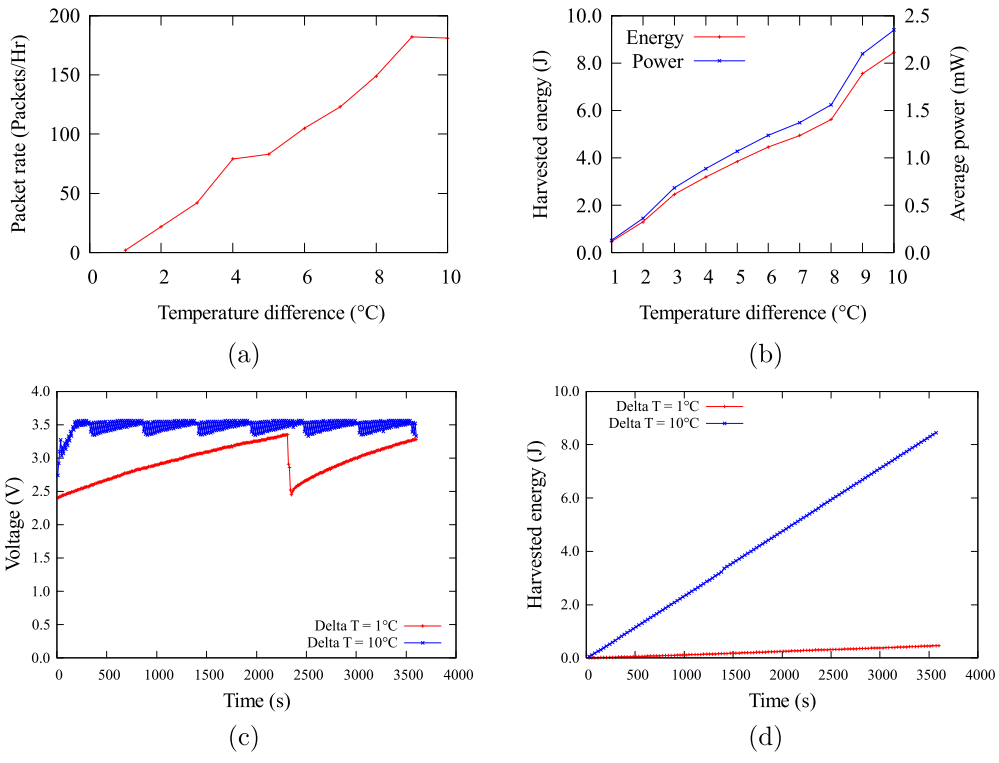

Fig. 14. Results produced by TEGBed for the experiments with batteryless DASH7 device. (a) achieved packet transmission rate (b) total harvested energy and average power (c) comparison of voltages of the energy buffer C_{STORE} for temperature difference 1 °C and 10 °C (d) comparison of energy accumulated over time for temperature difference 1 °C and 10 °C.

the device will stay in sleep mode and transmit a packet every 20 s. For every experiment, C_{STORE} was initially charged to, 2.5 V to ensure even conditions across the experiments.

The results derived from the experiments are presented in Fig. 14. We observe that the batteryless device can work even with temperature differences as low as 1 °C. However, from Fig. 14(a), when the temperature difference is 1 °C, the maximum packet rate achieved is only two packets per hour compared to the expected rate of 180 packets per hr. As shown in Fig. 14(b), during the one-hour emulation period, the system harvested 0.466 J energy with an average power of 0.129 mW. The energy yield increased to 8.45 J with an average power of 2.34 mW when the temperature difference increased to 10 °C. Furthermore, the system requires at least 9 °C temperature difference to keep the expected packet rate of 180 packers per hr or one packet every 20 s.

At 1 °C temperature difference, it took 2100 s to charge C_{STORE} from V_L to V_H. Where as at 5 °C, only 60 s were needed to charge C_{STORE} to V_H once discharged to V_L. For temperature differences above 9 °C, the harvester can provide enough energy to the storage buffer to keep its voltage always above V_L, thus allowing the target device to be always on. The batteryless node consumes

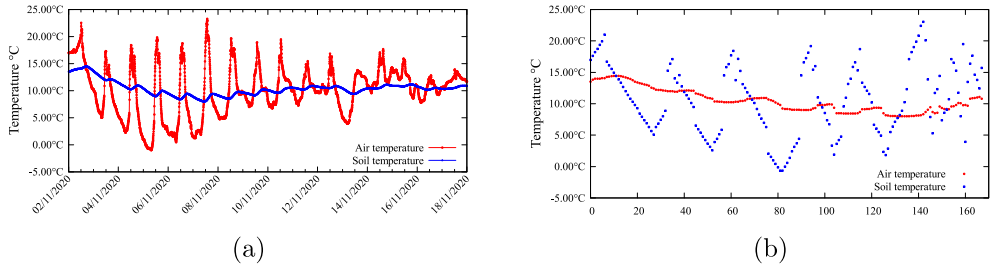

Fig. 15. Soil temperature and air temperature data collected from the University of Antwerp CDE campus from 02/11/2021 to 18/11/202 (a) whole data set (b) data set compressed into 168 unique soil and air temperature pairs using the data deflator.

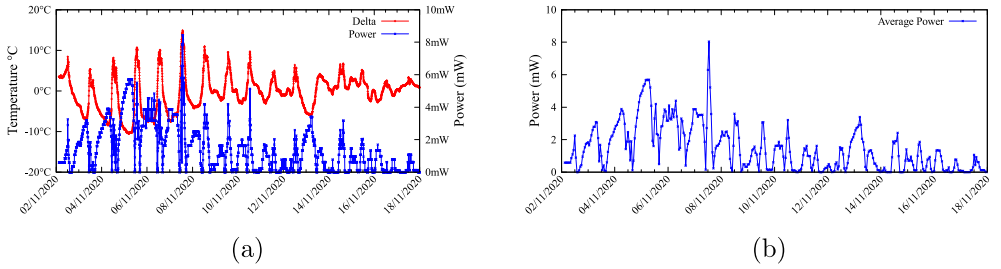

Fig. 16. Results produced by TEGBed for the emulation experiments conducted for the data collected from the CDE campus of the University of Antwerp from 02/11/2020 to 18/11/2020 (a) temperature delta and power difference (b) average power output per hour.

an average current of 12.69 mA for 509.5 ms to perform sensing and transmission. After transmission is performed, the device goes to sleep where the current consumption is 100 μA. Hence, went the temperature difference is 1 °C, the battery can supply the node for around 30 s before the battery voltage reaches below V_L.

4.3. Energy harvesting from soil and ambient air temperature difference

Thermoelectric generators are capable of converting temperature differences across them into electrical energy, making them suitable for any application where temperature differences can be generated. Soil thermal energy is an underutilized source of energy for batteryless and energy-harvesting designs. In recent times, researchers have started exploring the feasibility of scavenging energy from the temperature difference between air and soil [30,37,38]. This is possible since the soil temperature changes relatively slowly compared to the air temperature. This creates a consistent temperature difference between the soil and air. By harnessing energy from these temperature differences, many outdoor IoT devices can be powered sustainably and autonomously. In this section, we discuss how TEGBed can be used to assess the feasibility of generating energy from the temperature imbalance between soil and air. We use TEGBed to replay the data collected from the Campus Drie Eiken of the University of Antwerp in Belgium. The data collected contains air and soil temperatures sampled every 5 min from 2-11-2021 to 18-11-2021, for 17 days. The air temperature was measured using SHT31 A temperature sensor [39]. Soil temperature at a depth of 15 cm was measured using DS18B20 temperature sensor [40]. Fig. 15(a) shows a plot of the soil temperature and air temperature data collected.

The TEGBed could be used to replay the whole data set recorded from the field for 17 days. However, if replayed with the same sampling rate, the experiment would take 17 days to complete. So, to reduce the emulation time, one may reduce the sampling time. Nonetheless, it is not possible to reduce the sampling rate below 1 min, since the TEGBed needs a resting time of 1 min between every temperature set point. Therefore, an alternative option is to reduce the size of the data set. On evaluating the data sets, we observed that there are many repeating values for both the soil and air temperatures. So, we may divide the entire data set into different groups of repeating pairs of soil temperature and air temperature. We can emulate only these repeating pairs using TEGBed, and use the results to examine the whole data set. The data deflator is meant for this purpose. A tolerance of ±0.5° was allowed for the pairs. The deflator converted the data set with 4018 rows to a compressed set with 168 unique data points. The compressed data set is shown in Fig. 15(b). Once we have the numbers for the generated power for each temperature pair, we can calculate the per-day power output by counting the number of pairs each day and multiplying it with the recorder power values. This process is accomplished with the data inflator.

The data set shown in Fig. 15(b) was fed to the TEGBed and emulated to estimate the output power production. It took 9 h and 34 min for the TEGBed to emulate the 168 data points. For every data point, the energy and power generated were calculated. The results generated from the experiment are shown in Fig. 16. The power generated for each temperature difference is depicted in Fig. 16(a). The hourly average of the power is shown in Fig. 16(b). The TEGBed recorded a maximum power output of 8.41 mW

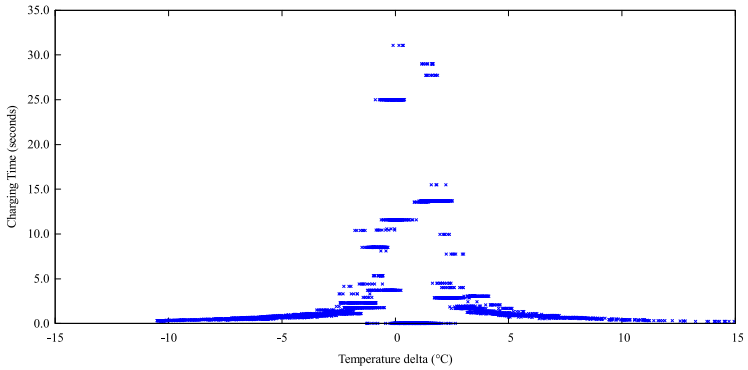

Fig. 17. The time taken by the Joule Counter to charge its capacitor (E_{STORE} = 720.51 μJ) for different temperature differences in the data collected from the CDE campus.

Table 2
LPWAN standards and energy consumption.

Standard	Activity	Energy consumption (mJ)
DASH7	A LOW_RATE device Transmitting 6 bytes in PUSH mode with Tx power = 14 dBm	12.64
LoRaWAN	Class A device with SF = 9 transmitting 6 bytes	43.95
NB-IoT	Transmission of 6 bytes	63.48
	Initialization, activation and connecting	3247.68

when the temperature difference was 14.94 °C. For the 17 days of data emulated, the average power output per day is 0.89 mW with an average temperature gradient of 3.40 °C.

A plot of charging time and temperature gradient is shown in Fig. 17. The charging time corresponds to the time taken by the Joule Counter to charge its capacitor from 1.25 V to 3.1 V, In other words, it is the time taken by the energy harvester to produce 720.51 μJ at different temperature differences. By using this plot, one can assess the time required to produce enough energy to power specific circuits at different temperature gradients. For instance, to power a device that consumes 500 mJ, it would take at least 285 s, when subjected to a temperature gradient of 4 °C. Therefore, by using these values, one can evaluate the feasibility of using soil thermal energy for different applications.

Powering batteryless LPWAN devices with soil thermal energy: Harvesting soil thermal energy opens up the possibility of making a myriad of outdoor IoT applications sustainable and energy-autonomous. Soil thermal energy can be used effectively in many situations where alternate resources such as solar or wind are impractical. Or, it could be used as a secondary source of energy to provide backup to the system when the primary source fails.

With the results obtained from emulation, we examine the possibility of designing batteryless IoT devices with different LPWAN technologies for data dissemination. We further use the results from our previous work on estimating the energy efficiency of LPWAN standards [41] to support our analysis. Our work in [41] presents a comprehensive analysis of energy consumption of different LPWAN standards and is summarized in Table 2. Utilizing these data, we estimate the minimum temperature difference required to power batteryless devices when using each LPWAN technology. Further, we examine how the size of the energy buffer impacts the performance of batteryless devices at different temperature differences and harvesting power.

We have the charging time measured by the Joule Counter for different temperature gradients as shown in Fig. 17. In addition to this, the energy required for different LPWAN technologies for transmitting a packet of 6 bytes long is available from [41] which is shown in Table 2. Based on these two data sets, it is possible to get a primitive idea about the feasible packet rate for a batteryless architecture for each LPWAN standard. The batteryless device as shown in Fig. 11(a) is turned on every time there is enough energy to perform a transmission of 6 bytes and powered off once the energy goes below the predefined thresholds. We assume a minimum possible value of C_{STORE} and V_L, meaning that every time the capacitor charges to V_H, it stores enough energy to perform at least one transmission task and discharges down to 0 V. The value of C_{min} for each standard can be calculated using Eq. (5). It is relevant to mention that, Eq. (4) does not consider the energy loss or difference due to variation in energy storage capacity of supercapacitors with charging and discharging currents [42]. Using Eq. (4), and the charging time measured for different delta, we can estimate the achievable packet rate for each LPWAN technology at different temperature gradients. We assume that a node will immediately wake up once the threshold is reached, perform a transmission of 6 bytes, and then go back to sleep or get powered off, as shown in Fig. 11(b).

Fig. 18, shows packet rates possible for different LPWAN standards when scavenging energy at different temperature gradients. We observe that with a temperature difference of 1 °C, a batteryless DASH7 node can perform transmission of 6 bytes every 103 s or achieve a packet rate of 35 packets/hr, a LoRaWAN node can achieve a packet rate of 10 packets/hr, and an NB-IoT node can achieve a packet rate of 7 packets/hr. At a temperature gradient of 20 °C, the achievable packet rate is 2387 packets/hr for DASH7, 692 packets/hr for LoRaWAN, and 480 packets/hr for NB-IoT. It must be noted that we have only considered the energy

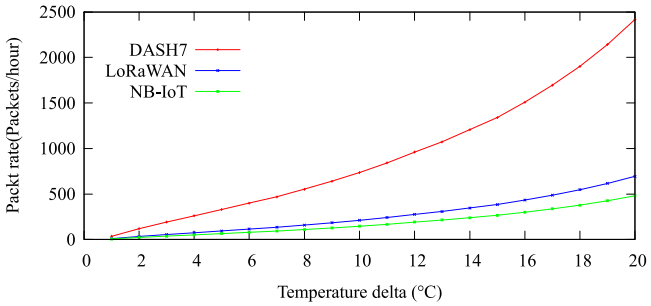

Fig. 18. Feasible packet rates for different LPWAN standards with thermal energy harvesting at different temperature gradients varying from 1 °C to 20 °C.

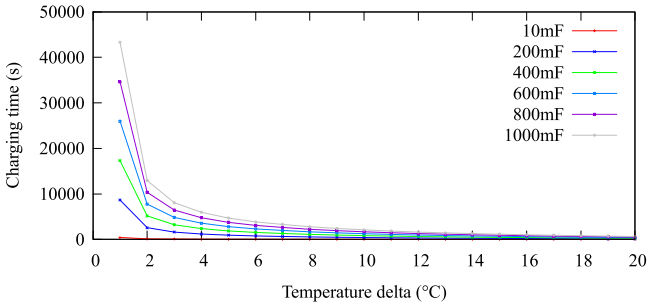

Fig. 19. Charging time for C_{STORE} varying from 10 mF to 1000 mF at different temperature gradients from 1 °C to 20 °C.

consumption during the transmission phase of the NB-IoT for the analysis presented in Fig. 18. But, if we assume that the NB-IoT performs the entire sequence of communication that includes, initialization, activation and connecting with the network, before each packet transmission, the feasible packet rate will be significantly reduced.

The results presented in Fig. 18 are based on the assumption that we choose a minimum capacitance for each standard and there is only one task to be executed by the device. A minimum capacitance for every LPWAN standard can be calculated based on the data presented in Table 2 and Eq. (5). Though this is the easiest approach, this could lead to the delayed execution of some of the tasks despite having enough energy in the buffer [43]. For instance, in Fig. 18, we calculated the feasible transmission interval for NB-IoT considering only the energy consumption during the data transmission process. However, before a packet transmission can happen over NB-IoT, there are exchanges of many control and synchronizing packets between the module and the base station. If we consider all these energy states, the total energy consumed by the module from waking up to sending a packet will be 3.21 J [41]. Using this energy value in Eq. (5), will give us the minimum capacitance as 900 mF, assuming $V_H = 3.3$ V, $V_L = 1.8$ V and $\eta = 90\%$. A plot of charging time for various capacitors at different temperature gradients is shown in Fig. 19. The packet rate is solely decided by the charging time when $C_{STORE} = c_{min}$. Thus, the feasible packet rate is around 6 packets per hr when the temperature difference is 20 °C and one transmission every 649 min or one every 10 h at 1 °C. Therefore, choosing a capacitor solely based on the peak energy consumption can adversely affect the performance of the batteryless systems in low energy harvesting conditions. This causes starvation low energy tasks despite having an ample amount of energy in the buffer to execute them. Consequently, a single storage buffer may not be an apt solution for many batteryless designs [43,44]. Further, it is worth noting that the results presented in Fig. 19 are based on the energy harvested by LTC3109 thermal energy harvesting PMIC which has relatively low efficiency. The datasheet reports a maximum efficiency of 35% for input voltages between 100 mV and 200 mV [29].

4.4. Energy harvesting from ambient and greenhouse temperature difference

Greenhouses are specialized farming environments that are built to grow crops within a controlled microclimate. They are designed to maintain optimum conditions that enhance crop growth. Consequently, the temperature inside a greenhouse can be significantly different compared to the ambient temperature outside. This temperature difference between the inside and outside of a greenhouse presents a valuable opportunity for energy harvesting. By harnessing the temperature differences, energy can be extracted and converted into usable power for various applications within the greenhouse. We collected temperature data [45] from one of the greenhouses at the Proefcentrum Hoogstraten [46] for a period of one month starting from 01-08-2022. The collected data include temperatures inside and outside the greenhouse. The temperature data were collected every 5 min and stored. A plot of recorded data points is shown in Fig. 20(a). The data deflator further converted this data set into a compressed set of 249 points which is presented in Fig. 20(b). The TEGBed was then used to emulate the temperature gradients and to measure the energy and power output.

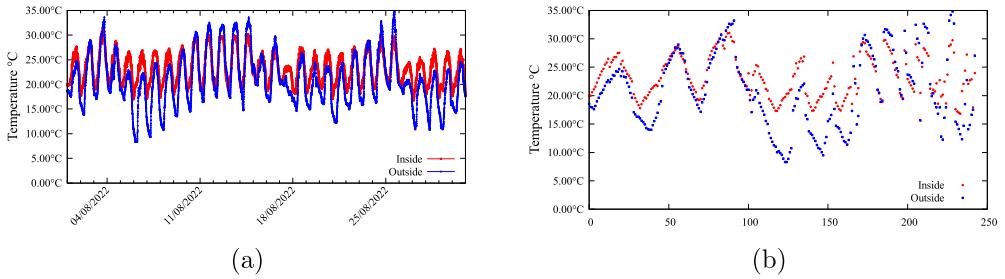

Fig. 20. Inside temperature and outside temperature of a greenhouse collected from the greenhouse at the Proefcentrum Hoogstraten from 01/08/2022 to 31/08/2022 (a) whole data set (b) data set compressed into 149 unique temperature pairs.

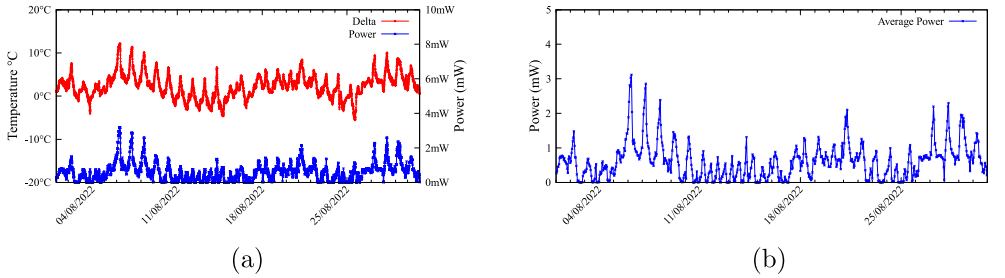

Fig. 21. Results produced by TEGBed for the emulation experiments conducted with the greenhouse temperature data. (a) temperature delta and power output (b) average power output per hour.

The results generated by the TEGBed are depicted as graphs in Fig. 21. A plot of the temperature difference and generated power for each difference is shown in Fig. 21(a). From the results obtained, we infer that the greenhouse data produced an average power of 0.60 mJ daily at an average temperature difference of 2.55 °C. An hourly average of the generated power is shown in Fig. 21(b). During the experiment, the TEGBed recorded a maximum power of 3.17 mJ for a temperature difference of 8.9 °C. Though it is evident that the power produced is considerably lesser than that for the soil temperature data, it must be taken into account that the data were collected during the summer, when the temperatures inside and outside the greenhouse were nearly equal. The plot in Fig. 20(a) justifies this. As a result, the temperature difference is less, hence the power generated. However, an improvement in the produced energy can be expected during winter when the outside temperature drops considerably. Since the greenhouse has to optimally maintain above 22.00 °C for most of the crops, a significant temperature difference can be achieved resulting in increased power output.

5. Discussions and future work

We presented a detailed discussion of TEGBed an automated test bed designed specifically for batteryless devices scavenging energy from heat. The TEGBed can serve as a valuable tool for conducting in-house evaluations of thermal energy harvesting devices, enabling researchers to conduct real-life simulations in controlled environments. TEGBed differs from other testbeds and emulators available in the scientific literature with its exemplary architecture and the micro-joule gauging tool Joule Counter. For instance, the work in [7] presents a testbed which can be used for characterizing TEG modules. The testbed provides a tool to measure the matched load output and to estimate the figure of merit of a TEG. However, the tool relies on the software tool LabVIEW to automate the tests and to acquire measurements. Moreover, the testbed is mainly meant to characterize a TEG module and hence not useful in the development and testing of batteryless devices. A similar architecture is presented in [6] which again concentrates on the characterization of TEG modules. Many such testbed architectures where the primary focus is on characterizing the TEG modules are available in the literature [5,47]. An architecture similar to TEGBed is discussed in [20] which uses an environment simulator for both thermal and solar energy harvesters. However, the testbed lacks an energy gauging tool like Joule Counter which can accurately estimate the power and energy output from the energy harvesting power management unit. Instead, the testbed uses a fake-load called *SmartLoad* architecture to emulate the current profiles of the IoT devices.

The distinguishing factor between TEGBed and other similar architectures available in the scientific literature is the introduction of a novel energy gauging tool, Joule Counter which uses simple yet accurate circuits for energy gauging. In addition, the components of the TEGBed do not rely on any expensive hardware or software but instead use readily available commodity items. This makes TEGBed easy to replicate and use or modify TEGBed to meet any custom testing conditions.

We elaborate on our plans for further enhancements to TEGBed and the limitations of the current version below.

Future Work: The TEGBed is currently in its early stage of development, and we anticipate continuous improvement by adding new features to increase its capabilities. As the technology of batteryless systems and energy harvesting are approaching new dimensions, it is important to ensure that TEGBed can serve a wide range of applications across different domains. Real-time energy-aware schedulers are increasingly becoming popular these days which can enhance the performance of batteryless systems based on different real-time conditions including energy availability, energy requirement, task priority, etc. [32,33]. We expect TEGBed to assist researchers in evaluating their real-time energy-aware schedulers. By utilizing TEGBed's ability to generate various temperature gradients and to measure produced energy in real-time, one can test their architecture against worst-case and best-case scenarios. The outcomes of these experiments can be further used to tune the performance of schedulers or software architectures. In addition to evaluating real-time schedulers, TEGBed may be used for testing energy prediction algorithms and low-power machine learning algorithms. Nonetheless, these use cases require TEGBed to measure both the energy input as well energy consumption by the target in realtime. The present architecture only allows for measuring the input energy using a Joulescope. While the energy consumption of the target can be easily measured by adding another Joulescope, this will significantly escalate the cost of TEGBed. To overcome this issue, we are actively working on designing energy measurement tools that can replace Joulescope. Further, once a stable version is achieved we will release the hardware architectures and firmware of the TEGBed as open-source so that the research community replicate and use it. By releasing the design of TEGBed as an open-source we expect to increase its visibility among the research community. In addition, improvements and add-on features are encouraged to enhance the performance of the testbed.

The selection of the right value for the energy buffer is a crucial aspect of any batteryless system design. In Section 4.2, we showed how we can estimate the approximate capacity required for the energy buffer using the knowledge of peak energy consumption. However, this is valid only in systems where the tasks are executed sequentially once powered on. As discussed in Section 4.3, the selection of capacitor based on Eq. (5) can adversely affect the performance of the system when there are multiple tasks with varying energy consummations are involved. It is even possible that the system uses multiple capacitors with different energy capacities to cope with the operating conditions [44]. For instance, when there are many choices for the storage buffer available on-board, a relatively small buffer can be used to charge at a low energy harvesting rate and some of the tasks may be executed using this energy [44]. Hence, the value of the energy buffer depends on the energy requirement of the target and energy availability from the harvester. The TEGBed can be used to evaluate the system under various energy harvesting conditions and storage buffers. However, an enhanced version would be able to capture the realtime behaviour of the harvester and provide valuable recommendations on the size and configuration of the storage buffer. We are currently exploring solutions that can enable TEGBed to generate insightful suggestions about the optimal value(s) for the storage buffer. Currently, the TEGBed does not do any data cleaning or filtering before the data is fed into the temperature emulator. Thus, we expect the data set (provided in the CSV file) to be free of any errors and duplicate series. However, this may not be true in many data sets. The data sets may contain unwanted data and incorrect data. Hence, we will look into the feasibility of implementing data filtering and cleaning tools as a part of the EC.

Limitations: Although TEGBed can emulate various real-life energy harvesting situations, there are some drawbacks and limitations that restrict its application in certain contexts. Currently, we use direct-to-air temperature generators for creating temperature differences. The direct-to-air temperature generators use heat conduction to heat or cool the point of contact. Though, it is true that the energy generated by the TEG modules is proportional to the temperature difference across them, the heat dissipation mechanism used with the TEG can impact the power output of the generator. Since TEGBed uses forced conduction, the impacts of heat-dissipating systems are disregarded. While this does not limit the application of TEGBed in evaluating various systems, it is important to note that results may have slight deviations from the actual values. Moreover, to emulate the impact of temperatures such as air temperatures which are often influenced by solar radiation, it might be more practical to integrate a thermal radiator as well to the testbed design. In addition to this, we currently use temperature generators that can provide or remove a maximum heat power of 30 W at room temperature. Thus, the temperature differences that can be achieved with these modules are limited and depend on the air temperature of the surroundings. We observe that the maximum difference we could achieve at 0 °C is 20 °C. This makes TEGBed unsuitable for emulating certain use cases where considerably high-temperature gradients are present. However, by replacing the existing temperature generators with higher-capacity generators we can overcome this limitation.

The Joule Counter which is a crucial component of the TEGBed employs simple yet efficient architecture to measure the energy production capacity of the harvesting system. At present, the design uses a pair of ceramic capacitors and a time base generated by a microcontroller to gauge energy production at different temperature gradients. While the approach is cheap and relatively easy to build, there is a concern regarding the long-term performance of the system. This arises since the capacity of ceramic capacitors can potentially degrade over time due to factors such as temperature and bias voltage. The currently used capacitor has a tolerance of ± 20 making its performance susceptible to circuit design and operating consideration. Moreover, the internal clocks of the microcontroller may exhibit variations over time and temperature. Considering these factors, the Joule counter may need calibration for each specific operating condition. Therefore, we plan to substitute the time base and capacitors with more precise components, thereby reducing measurement errors and eliminating the need for frequent re-calibrations.

6. Conclusions

Our work on TEGBed and the accompanying software and hardware tools present a comprehensive testbed solution for testing and evaluating batteryless devices in the IoBT domain. A novel sub-milliwatt energy measurement tool, Joule Counter enables accurate gauging of the energy production capacity of harvesters under different conditions. The temperature emulators allow precise examination of batteryless devices under different energy harvesting conditions. By providing realistic temperature gradients and energy yield assessment capabilities, this test bed opens up new possibilities for optimizing the design and performance of batteryless devices, leading to advancements in the field of IoBT and energy harvesting.

CRediT authorship contribution statement

Priyesh Pappinisseri Puluckul: Data curation, Formal analysis, Investigation, Methodology, Validation, Writing – original draft, Writing – review & editing. **Ritesh Kumar Singh:** Investigation, Writing – original draft, Writing – review & editing. **Maarten Weyn:** Supervision.

Declaration of competing interest

The authors declare the following financial interests/personal relationships which may be considered as potential competing interests: Priyesh Pappinisseri Puluckul reports financial support was provided by EU Horizon 2020 Research and Innovation Program.

Data availability

Data will be made available on request.

Acknowledgements

This research has received funding from the European Union's Horizon 2020 research and innovation program under the Marie Sokolowski-Curie grant agreement No 813114.

References

[1] F. Javed, M.K. Afzal, M. Sharif, B.-S. Kim, Internet of things (IoT) operating systems support, networking technologies, applications, and challenges: A comparative review, IEEE Commun. Surv. Tutor. 20 (3) (2018) 2062–2100, http://dx.doi.org/10.1109/COMST.2018.2817685.

[2] A. Raj, D. Steingart, Review—Power sources for the Internet of Things, J. Electrochem. Soc. 165 (8) (2018) B3130, http://dx.doi.org/10.1149/2.0181808jes.

[3] EnABLES, Research infrastructure to power the Internet of Things, 2017, https://www.enables-project.eu/wp-content/uploads/2021/02/EnABLES_ResearchInfrastructure_PositionPaper.pdf [Online; accessed 6-July-2023].

[4] D. Champier, Thermoelectric generators: A review of applications, Energy Convers. Manage. 140 (2017) 167–181, http://dx.doi.org/10.1016/j.enconman.2017.02.070, URL https://www.sciencedirect.com/science/article/pii/S0196890417301851.

[5] A. Ostrufka, E. Filho, A. Borba, A. Spengler, T. Possamai, K. Paiva, Experimental evaluation of thermoelectric generators for nanosatellites application, Acta Astronaut. 162 (2019) 32–40, http://dx.doi.org/10.1016/j.actaastro.2019.05.053, URL https://www.sciencedirect.com/science/article/pii/S0094576519302097.

[6] C. Izidoro, O. Ando Junior, J. Carmo, L. Schaeffer, Characterization of thermoelectric generator for energy harvesting, Measurement 106 (2017) 283–290, http://dx.doi.org/10.1016/j.measurement.2016.01.010, URL https://www.sciencedirect.com/science/article/pii/S0263224116000117.

[7] C. Guarnieri Calò Carducci, M. Spadavecchia, F. Attivissimo, High accuracy testbed for thermoelectric module characterization, Energy Convers. Manage. 223 (2020) 113325, http://dx.doi.org/10.1016/j.enconman.2020.113325, URL https://www.sciencedirect.com/science/article/pii/S0196890420308633.

[8] S. Vostrikov, A. Somov, P. Gotovtsev, M. Magno, Comprehensive modelling framework for a low temperature gradient thermoelectric generator, Energy Convers. Manage. 247 (2021) 114721, http://dx.doi.org/10.1016/j.enconman.2021.114721, URL https://www.sciencedirect.com/science/article/pii/S0196890421008979.

[9] T. Sanislav, G.D. Mois, S. Zeadally, S.C. Folea, Energy harvesting techniques for internet of things (IoT), IEEE Access 9 (2021) 39530–39549, http://dx.doi.org/10.1109/ACCESS.2021.3064066.

[10] K.Z. Panatik, K. Kamardin, S.A. Shariff, S.S. Yuhaniz, N.A. Ahmad, O.M. Yusop, S. Ismail, Energy harvesting in wireless sensor networks: A survey, in: 2016 IEEE 3rd International Symposium on Telecommunication Technologies (ISTT), 2016, pp. 53–58, http://dx.doi.org/10.1109/ISTT.2016.7918084.

[11] S. Zeadally, F.K. Shaikh, A. Talpur, Q.Z. Sheng, Design architectures for energy harvesting in the Internet of Things, Renew. Sustain. Energy Rev. 128 (2020) 109901, http://dx.doi.org/10.1016/j.rser.2020.109901, URL https://www.sciencedirect.com/science/article/pii/S136403212030188X.

[12] M.E. Yuksel, H. Fidan, Energy-aware system design for batteryless LPWAN devices in IoT applications, Ad Hoc Netw. 122 (2021) 102625, http://dx.doi.org/10.1016/j.adhoc.2021.102625, URL https://www.sciencedirect.com/science/article/pii/S1570870521001517.

[13] M. Molefi, E.D. Markus, A. Abu-Mahfouz, Wireless power transfer for IoT devices - A review, in: 2019 International Multidisciplinary Information Technology and Engineering Conference (IMITEC), 2019, pp. 1–8, http://dx.doi.org/10.1109/IMITEC45504.2019.9015869.

[14] M. Boebel, F. Frei, F. Blumensaat, C. Ebi, M.L. Meli, A. Rüst, Batteryless sensor devices for underground infrastructure—a long-term experiment on urban water pipes, J. Low Power Electron. Appl. 13 (2) (2023) http://dx.doi.org/10.3390/jlpea13020031, URL https://www.mdpi.com/2079-9268/13/2/31.

[15] H. Liu, H. Fu, L. Sun, C. Lee, E.M. Yeatman, Hybrid energy harvesting technology: From materials, structural design, system integration to applications, Renew. Sustain. Energy Rev. 137 (2021) 110473, http://dx.doi.org/10.1016/j.rser.2020.110473, URL https://www.sciencedirect.com/science/article/pii/S1364032120307590.

[16] M.V. Lukowicz, T. Schmiel, M. Rosenfeld, J. Heisig, M. Tajmar, Characterisation of TEGs under extreme environments and integration efforts onto satellites, J. Electron. Mater. 44 (1) (2015) 362–370, http://dx.doi.org/10.1007/s11664-014-3206-2.

[17] I. Petsagkourakis, K. Tybrandt, X. Crispin, I. Ohkubo, N. Satoh, T. Mori, Thermoelectric materials and applications for energy harvesting power generation, Sci. Technol. Adv. Mater. 19 (1) (2018) 836–862, http://dx.doi.org/10.1080/14686996.2018.1530938, arXiv:https://doi.org/10.1080/14686996.2018.1530938 PMID: 31001364.

[18] V. Leonov, Thermoelectric energy harvesting of human body heat for wearable sensors, IEEE Sens. J. 13 (6) (2013) 2284–2291, http://dx.doi.org/10.1109/JSEN.2013.2252526.

[19] S. Vostrikov, A. Somov, P. Gotovtsev, Low temperature gradient thermoelectric generator: Modelling and experimental verification, Appl. Energy 255 (2019) 113786, http://dx.doi.org/10.1016/j.apenergy.2019.113786, URL https://www.sciencedirect.com/science/article/pii/S0306261919314734.

[20] L. Sigrist, A. Gomez, M. Leubin, J. Beutel, L. Thiele, Environment and application testbed for low-power energy harvesting system design, IEEE Trans. Ind. Electron. 68 (11) (2021) 11146–11156, http://dx.doi.org/10.1109/TIE.2020.3036222.

[21] M. Minakais, S. Mishra, J.T. Wen, L. Lagace, T. Castiglia, Design and instrumentation of an intelligent building testbed, in: 2015 IEEE International Conference on Automation Science and Engineering (CASE), 2015, pp. 1–6, http://dx.doi.org/10.1109/CoASE.2015.7294032.

[22] E.T. Limited, Thermoelectric cooling/heating assembly , direct to air 34w, 2023, URL https://www.europeanthermodynamics.com/products/thermoelectric-assemblies/direct-to-air-thermoelectric-assemblies/adaptive-thermoelectric-assembly-direct-to-air-34w-dt-ar-034-12, Online; accessed: 2023-05-06.
[23] E.T. Limited, Adaptive junior PID PWM thermal controller, 2023, URL https://www.adaptivete.com/products/adaptive-junior-pid-pwm-thermal-controller-2/, Online; accessed: 2023-05-06.
[24] STMicroelectronics, Ultra-low-power arm cortex-M0+ MCU with 192-Kbytes of flash memory, 32 MHz CPU, USb, 2023, URL https://www.st.com/en/microcontrollers-microprocessors/stm32l072cz.html, Online; accessed: 2023-05-06.
[25] T. Instruments, 10 PA, ultra low leakage and quiescent current, load switch with reverse blocking, 2023, URL https://www.vishay.com/en/product/66597/, Online; accessed: 2023-05-06.
[26] S. Electro-Mechanics, BestCap®: A new generation of pulse double layer capacitors, 2023, URL https://product.samsungsem.com/mlcc/CL32A227MQVNNN.do, Accessed: 2023-07-14.
[27] J. LLC, Joulescope JS110: Precision DC energy analyzer, 2023, URL https://www.joulescope.com/products/joulescope-precision-dc-energy-analyzer, Online; accessed: 2023-05-06.
[28] K. Technologies, N6705B DC power analyzer, modular, 600 W, 4 slots, 2023, URL https://www.keysight.com/be/en/product/N6705B/dc-power-analyzer-modular-600-w-4-slots.html, Online; accessed: 2023-05-06.
[29] A. Devices, LTC3109 auto-polarity, ultralow voltage step-up converter and power manager, 2023, URL https://www.analog.com/en/products/ltc3109.html, Online; accessed: 2023-05-06.
[30] P. Pappinisseri Puluckul, M. Weyn, Battery-less environment sensor using thermoelectric energy harvesting from soil-ambient air temperature differences, Sensors 22 (13) (2022) http://dx.doi.org/10.3390/s22134737, URL https://www.mdpi.com/1424-8220/22/13/4737.
[31] T. Shibata, Y. Fukuzumi, W. Kobayashi, Y. Moritomo, Thermal power generation during heat cycle near room temperature, Appl. Phys. Express 11 (2018) http://dx.doi.org/10.7567/APEX.11.017101.
[32] C. Delgado, J. Famaey, Optimal energy-aware task scheduling for batteryless IoT devices, IEEE Trans. Emerg. Top. Comput. 10 (3) (2022) 1374–1387.
[33] M. Karimi, H. Choi, Y. Wang, Y. Xiang, H. Kim, Real-time task scheduling on intermittently powered batteryless devices, IEEE Internet Things J. 8 (17) (2021) 13328–13342, http://dx.doi.org/10.1109/JIOT.2021.3065947.
[34] M. Weyn, G. Ergeerts, L. Wante, C. Vercauteren, P. Hellinckx, Survey of the DASH7 alliance protocol for 433 MHz wireless sensor communication, Int. J. Distrib. Sens. Netw. 2013 (2013) http://dx.doi.org/10.1155/2013/870430.
[35] T. Instruments, TLV3691 0.9-V to 6.5-V, nanopower comparator, 2023, URL https://www.ti.com/lit/gpn/tlv3691, Online; accessed: 2023-05-06.
[36] Kyocera, BestCap®: A new generation of pulse double layer capacitors, 2023, URL https://www.kyocera-avx.com/news/bestcap-a-new-generation-of-pulse-double-layer-capacitors/, Accessed: 2023-07-14.
[37] N. Ikeda, R. Shigeta, J. Shiomi, Y. Kawahara, Soil-monitoring sensor powered by temperature difference between air and shallow underground soil, in: Proceedings of the ACM on Interactive, Mobile, Wearable and Ubiquitous Technologies, Vol. 4, Association for Computing Machinery, 2020, http://dx.doi.org/10.1145/3380995.
[38] Y. Tian, X. Liu, F. Chen, Y. Zheng, Harvesting energy from sun, outer space, and soil, Sci. Rep. 10 (2020) http://dx.doi.org/10.1038/S41598-020-77900-7.
[39] Sensiron, ±2% Digital automotive-grade humidity and temperature sensor, 2023, https://sensirion.com/products/catalog/SHT31A-DIS-B/, Online; accessed: 2023-05-06.
[40] M. Integrated, Programmable resolution 1-wire digital thermometer, 2023, https://www.maximintegrated.com/en/products/sensors/DS18B20.html, Online; accessed: 2023-05-06.
[41] R.K. Singh, P. Puluckul, R. Berkvens, M. Weyn, Energy consumption analysis of LPWAN technologies and lifetime estimation for IoT application, Sensors 20 (2020) 4794, http://dx.doi.org/10.3390/s20174794, URL www.mdpi.com/journal/sensors, 2020, Vol. 20, Page 4794.
[42] C. Renner, V. Turau, K. Römer, Online energy assessment with supercapacitors and energy harvesters, Sustain. Comput.: Inform. Syst. 4 (1) (2014) 10–23, http://dx.doi.org/10.1016/J.SUSCOM.2013.07.002.
[43] J. Hester, L. Sitanayah, J. Sorber, Tragedy of the coulombs: Federating energy storage for tiny, intermittently-powered sensors, in: Proceedings of the 13th ACM Conference on Embedded Networked Sensor Systems, 2015, pp. 5–16.
[44] A. Colin, E. Ruppel, B. Lucia, A reconfigurable energy storage architecture for energy-harvesting devices, ACM SIGPLAN Not. 53 (2) (2018) 767–781, http://dx.doi.org/10.1145/3173162.3173210.
[45] R.K. Singh, M. Aernouts, M. De Meyer, M. Weyn, R. Berkvens, Leveraging LoRaWAN technology for precision agriculture in greenhouses, Sensors 20 (7) (2020) http://dx.doi.org/10.3390/s20071827, URL https://www.mdpi.com/1424-8220/20/7/1827.
[46] Proefcentrum, Proefcentrum hoogstraten, 2023, https://www.proefcentrum.be/, Online; accessed: 2023-05-06.
[47] P. Solanki, D. Deshmukh, V. Diware, M. Deshmukh, Experimental investigation of thermoelectric generator system, Mater. Today: Proc. 47 (2021) 3012–3017, http://dx.doi.org/10.1016/j.matpr.2021.05.478, URL https://www.sciencedirect.com/science/article/pii/S2214785321040803, 3rd International Conference on Advances in Mechanical Engineering and Nanotechnology.